Computational fluid dynamics calculations of binary representation of Ni-base superalloy solidification in frustum geometries

Allen, J D T; Green, N; Warnken, N

DOI:
10.1088/1757-899X/1274/1/012052

Document Version
Publisher's PDF, also known as Version of record

Computational fluid dynamics calculations of binary representation of Ni-base superalloy solidification in frustum geometries

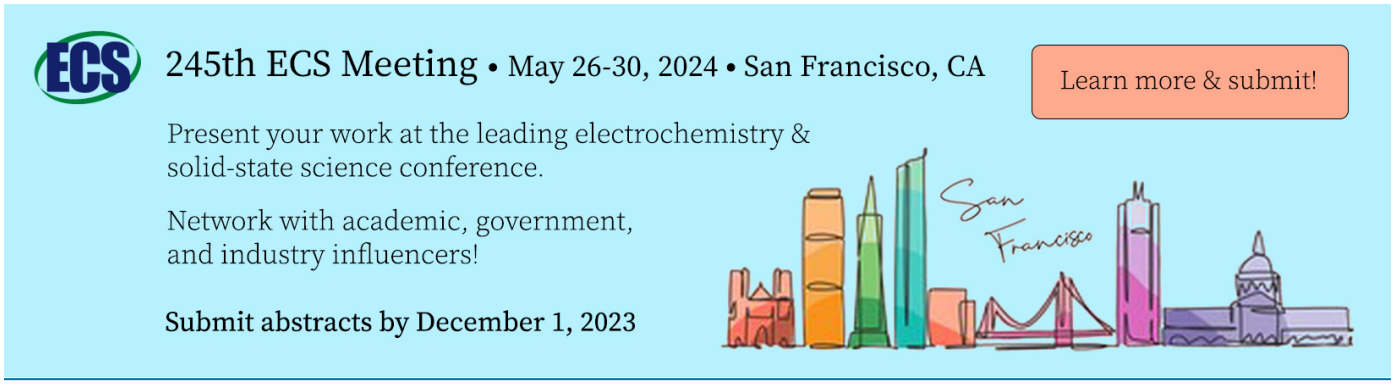

Computational fluid dynamics calculations of binary representation of Ni-base superalloy solidification in frustum geometries

J D T Allen[1], N Green[2] and N Warnken[1,3]

[1]University of Birmingham, School of Metallurgy and Materials, Edgbaston, Birmingham, England, B15 2TT
[2]High Temperature Research Centre, Airfield Drive, Coventry CV7 9BF

Abstract. CFD calculations were carried out on a number of frustum geometries from the experimental literature on freckling of superalloys. The effects of two imposed thermal fields were investigated, flat and inclined. Experiments document that when thermal fields are inclined the cold side is more prone to formation of freckles; our results conclude that rising liquid plumes in advance of the solidification front, which can correlate to freckles, are more abundant and intense on the cold side. Also, modelled plume activity is greater in inward sloping frustum geometries as opposed to outward sloping ones, which also agrees with established literature. Complex flow patterns were observed in inclined geometries and there is a clear interplay and competition between both the thermal and solutal aspects of flow, with flow being significantly changed, sometimes reversed in direction in some capacity. Our results also offer insight into the incubation length for plume and resultant freckle formation after the transition between frustums, with some critical distance of advance of the solidification front necessary to initiate and establish other plumes that feed into the main one circulating liquid flow which is locally intense enough to potentially create a freckle.

1. Introduction

The phenomenon of the freckle has been known about in the process of directional solidification for approximately 50 years and is significant to many areas of materials science including austenitic stainless steels, superalloys and in geothermal settings [1, 2, 3, 4, 5]. This paper is an investigation of the phenomenon in nickel-based superalloys. A freckle is a chain of small eqiuiaxed grains of random orientation on the surface of a casting [2, 6, 7]. In the scientific literature freckling is widely understood to be caused by the process of thermosolutal convection [7, 8, 9] which is caused when, during thermally constrained directional solidification, heavy elements (such as Re and W in superalloys) segregate to the dendrites, resulting in a layer of liquid of reduced density in the mushy zone [7, 8, 9]. In the mushy zone there are frictional and buoyancy forces active and should the buoyancy forces overcome the frictional forces plumes of liquid can emerge from the mushy zone [7]. These plumes can cause remelting of the secondary dendrite arms forming stable channels of intense and persistent flow allowing for the initiation of freckles during solidification [10, 11]. Freckles are highly significant in turbine applications. For nickel-based superalloys a single freckle can significantly reduce the mechanical properties, resulting in parts which are unfit for service as they cannot be post-hoc removed via mechanical or thermal treatments [1, 2, 12, 13, 14].

[3] Corresponding Author: N.Warnken@bham.ac.uk

There have been many factors identified to affect the possibility and severity of freckling, the first is alloy composition, adding heavy elements that are known to partition to the dendrites, for example Re and W, would worsen freckling, whereas adding heavy elements that are known to segregate to the interdendritic regions such as Ta, is known to reduce freckling [1, 7, 15]. In addition to this, the use of carbon to from carbides close to the liquidus also suppresses freckling [7, 8]. The second is thermal conditions, for example Schadt et. al. [16] found in general for an array of geometries for CMSX-4 that if the product of the two variables thermal gradient, *G,* and withdrawal velocity, *V,* was less than 0.14 K/s then freckles would likely occur. On the other hand, the work of Ma et. al. [17] analysed a single cylindrical geometry and concluded that there is a region of freckling at intermediate values of *G* and *V* with no freckling outside of that. The third is the thickness of the sample; it is known from the literature that a thicker sample has a longer mushy zone which increases the likelihood of freckling [7, 8, 12]. Finally, and most important to this paper, the geometric features; in many castings freckles are associated with a rapid increase or decrease in the thickness of a sample, or a surface that inclines inwards or outwards, the latter chiefly being the effect investigated in this paper [1, 12, 18, 19].

In the research of Ma et. al. [1, 12] several experiments and thermal field simulations have been carried out on geometries which have sloping surfaces either inwards or outwards [1, 12]. It was determined experimentally that inward sloping faces are more prone to formation of freckles than outward sloping faces [1, 12]. Ma et. al. made the determination that this was due to the reservoir theory [1, 12, 19]. In this reservoir theory a sufficient mushy zone reservoir of enriched liquid below a plume is required to feed it. The size of the reservoir is enhanced when the surface slopes inwards [1, 12]. In Ma's experiments, freckles were found in 2 scenarios, in the outward sloping cases some plumes were found at the transition between 2 frustums, and in the inward sloping cases more prominent plumes were found leading up to the transition points after an incubation height [1, 12]. The reason for the short plumes after the transition to a smaller diameter has been reasoned to be due to the step effect. Immediately after the transition, there is an existing reservoir (the mushy zone) and a newly obtained surface, allowing for a short freckle [1, 12, 20]. The incubation height is caused by the fact that after a cross-section transition to a larger diameter it requires a certain solidification distance to establish said reservoir again [1, 12, 18, 19]. In most castings radiation effects dictate that the thermal field is not perfectly horizontal. In the literature it is documented that freckles are more likely to appear on the cold side of the geometry, *i.e.* the most advanced portion of the advancing solidification front [20].

In this study CFD computer simulations are conducted on inward sloping and outward sloping geometry frustrums using both non-inclined and inclined thermal fields for the purpose of seeing where plumes local to the solidification front occur and whether they correspond to freckles in the experimental results [1, 12]. Both the composition field and flow field are analysed to this end.

2. Simulation

The model used is implemented in this study using the routine created by Crane and Coleman named solidificationFoam, that is implemented within the CFD package OpenFOAM. (https://github.com/OpenFOAM/OpenFOAM-Solidification). The model uses the pressure corrector algorithm SIMPLE, the details of which are explained elsewhere [24, 25]. The model uses 2 iteration loops, one for the temperature and composition and the other for flow velocity and pressure. One was set to be converged when the difference in solid fraction is less than $1 \cdot 10^{-4}$ and the other one was set to be converged when the difference in pressure is less than $1 \cdot 10^{-8}$ Pa. Non-slip velocity boundary conditions were used in all calculations.

Two geometries have been created based on those which feature in the research of Ma et.al. [12] which shall be called geometries G1 and G2 respectively, see Figure 1. In order to accurately assess the flow patterns at and near the surfaces of said geometries, the meshes were constructed as follows: within 4 mm of the surfaces, the maximum cell element volume is set to $6.4 \cdot 10^{-11} m^3$ ($0.4^3 mm^3$), the rationale behind this was it was necessary to have a cell size with lengths comparable to the primary dendrite arm spacing associate with thermally constrained directional solidification of nickel base superalloys. The meshes have larger elements in the core of the geometries to reduce the computational expense.

Two isotherm conditions were applied, horizontal and inclined at 15 degrees to the horizontal. Values for G and V were selected based on the literature, wherein previous research using these geometries selected a fixed V of 1 mm/min but various G values [1, 12]. These G values vary between 1000 K/m and 2900 K/m, the range of reported conditions having been determined by simulations or thermocouple measurements of the researchers [12]. In the end, the intermediate G value 1900 K/m was selected. G and V were then used to calculate the temperature on the surface of the metal as function of time and z-coordinate using the equations $min\{z_{dist} = z - (t \cdot V), 0\}$ and $T = T_{furn} + (G \cdot z_{dist})$ where t is the time, z is the z-coordinate of a point in a vertical frame of reference and T_{furn} is the furnace temperature 1773 K. This was then used a boundary condition for transient thermal fields inside the metal, as obtained from heat transport through conduction and convection.

The primary dendrite arm spacing was determined using the following equation $\lambda_1 = 2.83 \cdot (k \cdot \Gamma \cdot D_{liq} \cdot \Delta T)\ 2.83 \cdot G^{-0.5} \cdot V^{-0.25}$ where ΔT is the difference between T_{liq} and T_{sol}, k is the partition coefficient, Γ the Gibbs Thomson coefficient and D_{liq} the solutal diffusion coefficient in the liquid. This equation was created by Hunt by considering the geometry of cell/dendrite tip as a hemispherical cap and detailed in [21, 22]. Simulations were done using a pseudobinary representation of the commercial single crystal superalloys CMSX-4.

The second generation single crystal superalloy CMSX-4 is a widely used commercial single crystal superalloy, consisting of nine mayor elements. This alloy is well known as a freckle prone alloy and quite widely studied [1,16-20]. CFD simulations with this level of compositional complexity still provide a significant computational challenge. For this reason, a pseudo binary representation is commonly used in the superalloy solidification community, Ren et.al. [23] recently published work on CMSX-4 using this approach. A binary alloy consisting of nickel plus a fictitious second element is created, represented by a liquidus slope and partition coefficient – see Table 1 for data used in the present study, giving a useful representation on properties especially segregation behaviour, solidification range, effect of solute on liquidus temperature.

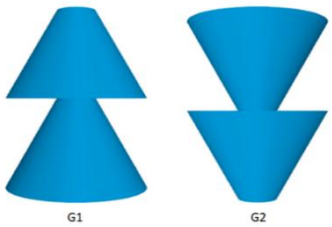

Figure 1: The two geometries used in the simulations, each individual frustum has a diameter of 30mm at its thickest point, a height of 15mm and a sloping angle of 30 degrees.

Table 1. Relevant quantities used in the simulations taken from [1]

Quantity	Value	Units
Latent Heat of Fusion	240000	Jkg^{-1}
Reference Density(ρ_{ref})	7646	kgm^{-3}
Nominal Composition of Solute(C_0)	38.2	wt%
Partition Coefficient(k)	0.6883	-
Solvent Melting Temperature(T_s)	1726	K
Heat Capacity(C_p)	575	$kJkg^{-1}$
Solid Thermal Conductivity (K_{ts})	24.6	WmK^{-1}
Liquid Thermal Conductivity (K_{tl})	33.5	WmK^{-1}
Reference Temperature(T_{ref})	1773	K
Eutectic Temperature (T_E)	1593	K

Quantity	Value	Units
Dynamic Viscosity (μ)	$4.93*10^{-3}$	$kgm^{-1}s^{-1}$
Liquidus Temperature Nominal (T_{liq})	1660.973	K
Solidus Temperature Nominal (T_{sol})	1631.523	K
Thermal Expansion Coefficient (β_T)	$1.16*10^{-4}$	K^{-1}
Solutal Expansion Coefficient (β_C)	$2.51*10^{-1}$	$wt\%^{-1}$
Solidus Slope (m_S)	-2.4732	$Kwt\%^{-1}$
Liquidus Slope (m_L)	-1.7023	$Kwt\%^{-1}$
Gibbs Thompson Coefficient (Γ)	$2.84*10^{-7}$	Km
Diffusion Coefficient in Liquid (D_{liq})	$3.60*10^{-9}$	m^2s^{-1}

3. Results and Discussion

Figure 2 documents the composition profile at or very close to the end of solidification. Segregation arises as a consequence of, and denotes, flow of partitioned solute enriched liquid plumes. Our results seem to align with the results of the previous literature, in that G1 with contracting frustums has a lot more plume activity than G2 with expanding ones [1, 12]. In all cases the composition of the alloying element increases relative to the nominal composition at and near the very top of the geometry. This is simply the result of the phenomenon of macrosegregation. With regard to the conditions with thermal fields inclined by 15 degrees, stronger plume activity on the cold side of the specimen accords with literature [20]. A series of plumes proceed upwards along the inclined front to feed a singular vertical plume at the point furthest away from the heating element/cooler face in the case of G1, this also aligns with literature data [1, 12]. In the case of G2 less intense plume activity is detected, although notably on the cold side a prominent plume appears just above the transition, this appears consistent with the experimental results where a freckle is often found just above the transition due to the step effect [1, 12].

Flow activity during solidification is summarised in Figure 3. Three snapshots at 3 different points during solidification for each calculation were taken when the solidification was half way up each frustum and at the union. The first important observation, that applies mostly to the results with inclined thermal fields, is that the intensity of flow is reduced as solidification proceeds, apparently due to reducing free liquid volume ahead of the solidification front. In cases without inclined isotherms this is less relevant, as flow is dominated by solutal effects.

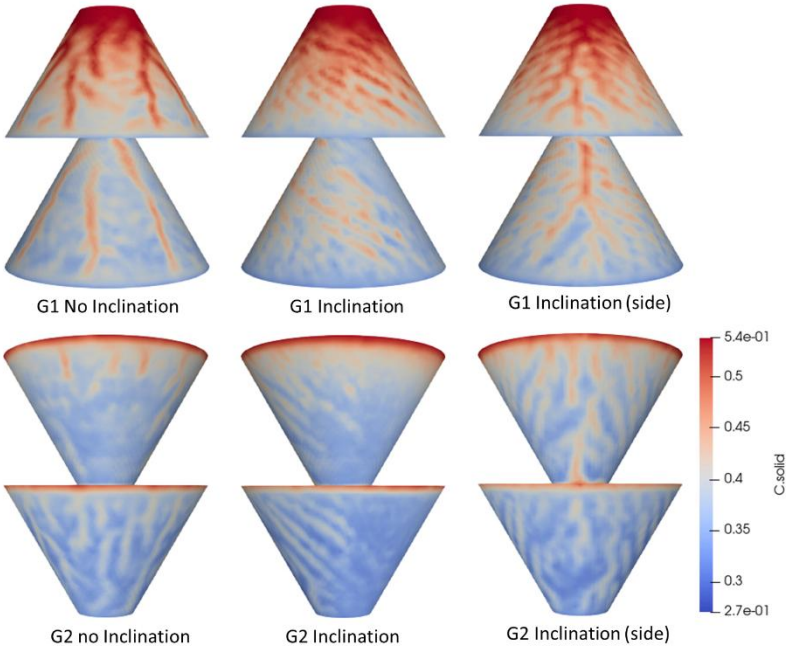

Figure 2. Solid composition profiles in the two geometries for both inclined and non-inclined temperature profiles. In inclined profiles the cold side is always to the left. In the side view the cold side faces the camera.

The second important observation arising from these results is that overall, there is more flow in the far field from the solidification front for cases where the thermal field is inclined. This is not only due to convection effects caused due to the thermal field, liquid on the hot side rising and that on the cold side falling but also as a consequence of more complex interactions arising from the differential distribution of the rising low density liquid ahead of the solidification front. In the lower frustrum of G1 geometry with the inclined front the flow is reversed based on what would be expected with thermal flow alone, indicating conditions where solutal flow is intense and likely to be favourable for freckle formation. However this does not occur in the G2 geometry in the bottom frustum due to the dissipative action of the expanding section leading to much weaker plume flow that could not overwhelm the thermal flow in this way. In the top frustum, due to the fact that the thermal flow is much weaker, we have a reversal effect. At the union also, due to the large plume there is also a reversal effect arising from momentum, but there is also a pocket of flow in the centre that follows the

thermal direction, indicating that the solutal flow is not fully yet dominant. In the cases with no inclination we typically see that there is very limited thermal flow (which would be expected to be down at surfaces up in the centre) allowing for a series of weaker plumes at the surface to proceed which have no factor driving them to merge like inclined cases.

A further key observation arising from this study is that the appearance of plumes does not necessarily correspond to the appearance of freckles, for example we see some plume activity in G2 inclined but no freckles experimentally (except for on the cold side just above transition) [12]. In the experimental literature freckles only occur in G1 after an incubation height of *5mm* from the transition [12]. In the example of G1 inclination (where the inclined thermal field serves as a first degree approximation of the experimental curved profile), there is no delay, but there is an incubation period before the main plume is being fed by a lot of others, of about the same length as observed experimentally, this could explain why there is an incubation zone. This observation does counteract the aforementioned reservoir theory, however it is clear that more research needs to be done in this regard.

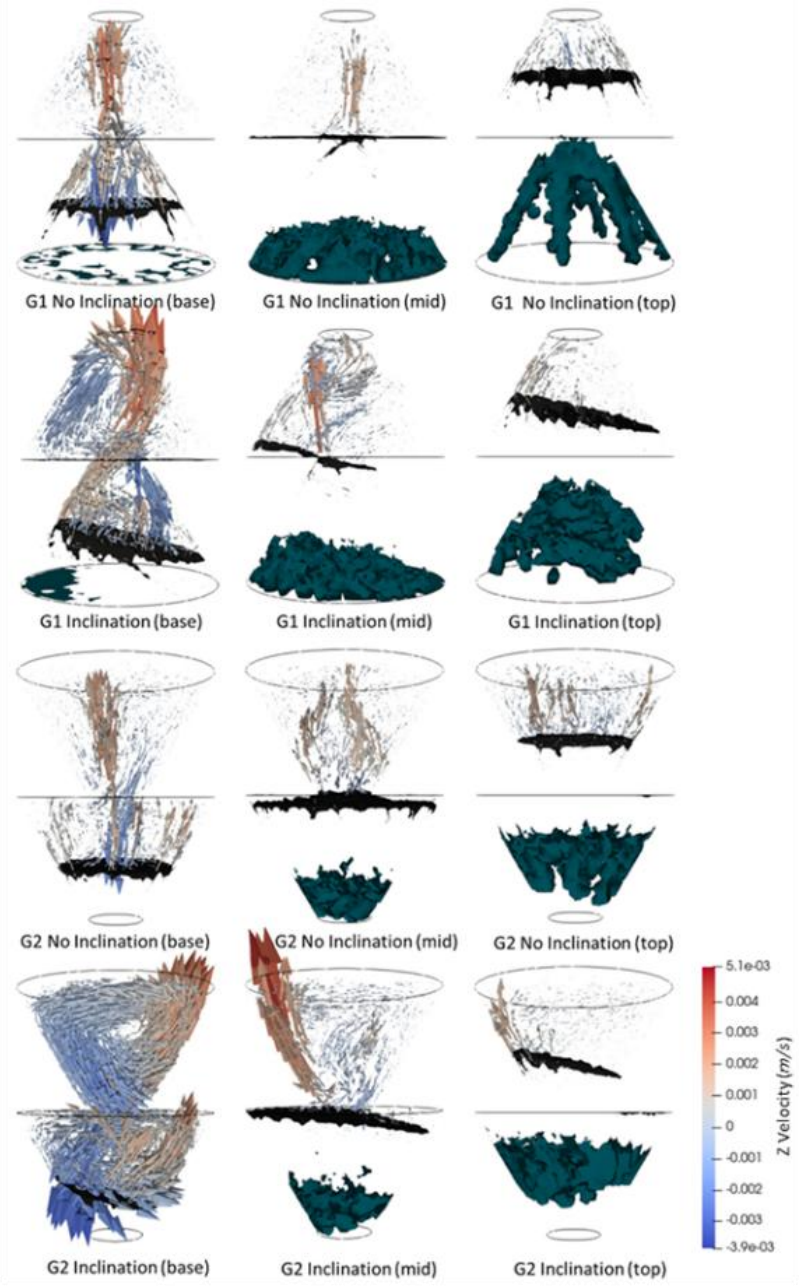

Figure 3. Velocity profiles in the two geometries as described in figure 1 for both inclined and non-inclined temperature profiles. In inclined profiles the cold side is always to the left. The green contour corresponds to full solidification and the black contour corresponds to 1% solidification. The coloring of the arrows is determined by the z-component of the flow vector the redder the more upwards the flow and the blue the more downwards.

4. Conclusions

- CFD computer simulations were designed to assess the effects of geometry and inclination of temperature profile on plume activity. Results showed that outward sloping geometries are less prone to plume occurrence than inward sloping geometries.
- In the case of an inclined temperature field the model indicated that the cold side is more susceptible to plume occurrence than the hot side.In inward sloping geometries the model predicted a series of plumes would combine into a single intense channel at the uppermost point of the advancing grain envelope.
- Computed flow patterns match the occurrence of freckles in the experimental data to which comparison was made.
- Complex flow patterns arising from coupled thermal and a solutal effects were observed in geometries with inclined profiles, with the solutal flow strongly impacting the overall flow in high plume situations, notably the inward sloping geometry.
- The appearance of plumes does not completely correspond to the occurrence of freckles, due to presence of an incubation height.

5. References

[1] Hong J, Ma D, Wang J, Wang F, Dong A, Sun B and Bührig-Polaczek A 2015 *J. Alloys Compd.* **648** 1076–82.
[2] Giamei A F and Kear B 1970 *Met. Trans.* **1** 2185–92.
[3] Fowler A C 1985 *IMA J. Appl. Math.* **35** 159–74.
[4] McKenzie D 1984 *J. Petrol.* **25** 713–65.
[5] Jacobs J A 1953 *Nature* **172** 297–98.
[6] Ren N, Panwisawas C, Li J, Xia M, Dong H and Li J 2021 *Acta Mater.* **215** 117043.
[7] Reed R C 2006 *The Superalloys*, (Cambridge University Press-Cambridge).
[8] Tin S and Pollock T 2003 *Metall. and Mater. Trans. A* **34** 1953–67.
[9] Tin S, Pollock T and Murphy W *Metall. and Mater. Trans. A* 2001 **32** 1743–53.
[10] Yuan Y and Lee P D 2012 *Acta Mater.* **60** 4917–26.
[11] Kao A, Shevchenko N, Alexandrakis M, Krastins I, Eckert S and Pericleous K 2019 *Philos. Trans. Royal Soc. A* **377** 20180206.
[12] Ma D and B¨uhrig-Polaczek A 2014 *Metall. and Mater. Trans. A* **45** 1435–44
[13] Yu K O, Domingue J A, Maurer G E and Flanders H D 1986 *JOM* **38** 46–50.
[14] Amouyal Y and Seidman D 2011 *Acta Mater.* **59** 6729–42.
[15] Amouyal Y and Seidman D 2011 *Acta Mater.* **59** 3321–33.
[16] Schadt R, Wagner I, Preuhs J and Sahm P 2000 *Superalloys 2000: Proc. of the 9th Int. Symp. on Superalloys* T M Pollock (Minerals, Metals and Materials Society- Pennsylvania) 211– 8
[17] Ma D, Zhou B and Bührig-Polaczek A 2011 *Adv. Mat. Res.* **278** 428–33.
[18] Ma D X, Mathes M, Zhou B and Bührig-Polaczek A 2011 *Adv. Mat. Res.* **278** 114–9.
[19] Ma D, Ziehm J, Wang W and Bührig-Polaczek A 2012 *Solidification and Casting of Metals*: *Proc. of an Int. Conf. on Solidification.* (Rolduc Abbey-Aachen) vol 27 012034.
[20] Ma D, Wu Q and Bührig-Polaczek A 2012 *Metall. and Mater. Trans. B* **43** 344–53.
[21] J. Hunt 1979 *Solidification and Casting of Metals*: *Proc. of an Int. Conf. on Solidification* (Metals Society-London) 3–9.
[22] Ghosh S, Ma L, Ofori-Opoku N and Guyer J E 2017 *Model. Simul. Mat. Sci. Eng.* **25** 065002.
[23] Ren N, Li J, Panwisawas C, Xia M, Dong H and Li J 2021 *Acta Mater.* **206** 116620
[24] Caretto L S, Gosman A D, Patankar S V and Spalding D B 1973 H Cabannes and R Temam (Springer-Berlin) *Proc. of the 3rd Int. Conf. on Numerical Methods in Fluid Mechanics* vol 2 60–8.
[25] Patankar S V and Spalding D B 1973 *14th Symp. (Int.) on Combustion*. (Pennsylvania State University-Pennsylvania) vol 14 605–14.